Neural Networks-Generalized Predictive Control for MIMO Grid-Connected Z-Source Inverter Model

Navid Salehi, Herminio Martinez-Garcia, Guillermo Velasco-Quesada
ELECTRONIC ENGINEERING DEPARTMENT, UNIVERSITAT POLITECTICA DE CATALUNYA – BarcelonaTech (UPC)
Escola d'Enginyeria de Barcelona Est (EEBE), Av. Eduard Maristany, nº 16. E-08019 Barcelona, Spain
Tel.: +34.93.413.72.90
E-Mail: navid.salehi@upc.edu, herminio.martinez@upc.edu, guillermo.velasco@upc.edu
URL: http://www.eel.upc.edu

Acknowledgements

The authors would like to thank the Spanish Ministerio de Ciencia, Innovación y Universidades (MICINN)-Agencia Estatal de Investigación (AEI) and the European Regional Development Funds (ERDF), by grant PGC2018-098946-B-I00 funded by MCIN/AEI/10.13039/501100011033/ and by ERDF A way of making Europe.

Keywords

«Z-source», «MPC», «GPC», «ANN», «Non-minimum phase», «MIMO»

Abstract

This paper presents a neural network-generalized predictive control (NN-GPC) for a single-phase grid-connected z-source inverter. The NN forecasts the predictive horizon, and the conventional GPC algorithm calculates the control horizon. The results verify the proposed NN-GPC effectively enhances the dynamic operation of z-source inverter regarding the non-minimum phase characteristics of these converters.

Introduction

As a sustainable solution to provide the world's electrical energy, distributed energy resources (DERs) integrated with renewable energies (REs) are strongly regarded by researchers. Inverters in microgrids (MGs) and DERs systems provide standard AC electricity for customers and play a special role in the stability and optimal operation of the system. By introducing the concept of impedance source converters, z-source inverters (ZSI) are investigated rapidly in order to improve their performance. ZSI proposes a single-stage inverter with inherent buck-boost ability due to implementing an impedance network into the DC link. Therefore, the ZSI can operate as a voltage source inverter (VSI) and current source inverter (CSI) simultaneously by controlling the duty cycle of the converter. Although the reliability, efficiency, and cost-effectiveness are improved in ZSI, some weak points led to the proposal of different impedance network topologies [1]. The main disadvantages of impedance source converters are the high current and voltage stress of the input rectifier diode and the inability to inject reactive power into the grid [2]. Various topologies are proposed to alleviate these weaknesses. However, inherently impedance source converters suffer from the mentioned problems. In [3], a modified cascaded Z-source high step-up boost converter is proposed in order to obtain a high conversion ratio with low voltage stress of semiconductor devices. In addition, the results verify that the proposed topology operates at continuous current mode (CCM) with low current and voltage stress.

The control techniques in ZSI are normally deployed to control the capacitor voltage and inductor current of the impedance network and the inductor current of the inverter's AC side. However, the control strategies in ZSI are a challenging issue due to the existing right-half-plane (RHP) zero into the control to capacitor voltage transfer function of the impedance network. Accordingly, different control strategies are adopted to ZSI as a non-linear and non-minimum phase system [4]. The proportional-integral-derivative (PID) controller can be applied to the ZSI to control the converter around a specific operating point. Therefore, the converter operation is restricted, and the converter dynamic is affected by operating point variation. In [5], a PID-like fuzzy control strategy is established to control the peak dc-link voltage. The PID parameters are determined according to the fuzzy logic-based rule sets. The rule sets in this paper are modified based on the trajectory performance of the phase plane in order to enhance the transient performance. Sliding mode control, fuzzy logic controller, model predictive control (MPC), and neural networks control are some other controllers that can effectively apply to the ZSI. In [6], a neural networks control technique is exploited to control DC boost and AC output voltage of ZSI. The space vector pulse-width-modulation (SVPWM) is modified in this paper in order to control the shoot-through (ST) duty ratio to boost dc voltage.

Model predictive control (MPC) is also widely applied to the ZSI control scheme. In [7], MPC predicts the capacitor voltage, inductor current, and output load current of a switched-inductor quasi ZSI to compare with the corresponding reference values. Then, the switching states are selected to achieve the minimum cost function. In [8], MPC is used in islanded and grid-connected operation modes to achieve a seamless transition between operation modes, fast dynamic response, and small tracking error under the steady-state condition of controller objectives. In [9], MPC is applied to the quasi ZSI to reduce the inductor current ripple and the output current error. In recent years, different MPC algorithms based on the predictive process model and defined cost function have been introduced. Dynamic matrix control (DMC) and model algorithmic control (MAC) are two MPC algorithms based on system step response and impulse response. Moreover, generalized predictive control (GPC), which is based on the system's discrete transfer function, and predictive functional control (PFC) based on the system's state space are two advanced MPC algorithms. Neural networks MPC (NN-MPC) can also be used specifically in complicated systems that conventional system identification methods such as step response, impulse response, transfer function, or state space of the system cannot be applied straightforwardly. The NN-based MPC algorithms are not fast due to high burden calculations. Therefore, NN-MPC is not developed in recent years compared to other MPC algorithms.

In this paper, neural networks GPC (NN-GPC) is applied to the ZSI in order to predict the capacitor voltage and inductor current of the impedance network and output inductor current. In this algorithm, the forced response of the predictive control is obtained by neural networks. The analysis shows that the proposed MPC algorithm enhances the dynamic response of the ZSI without increasing the calculation burdens. To verify the theoretical analysis, the simulation results are compared with conventional GPC. The rest of the paper is structured as follows. First, the multi-input multi-output (MIMO) model of the ZSI is presented. Then, by obtaining the discrete transfer functions of the ZSI, the proposed NN-GPC is introduced. Eventually, the simulation results are shown in order to verify the theoretical analysis.

MIMO z-source inverter model

As it can be seen from Fig. 1, the single-phase Z-source inverter consists of an impedance network and an H-bridge inverter. The impedance network involves two inductors L_1 and L_2, and two capacitors C_1 and C_2. In addition, a rectifier diode is in series with the input DC voltage source. The impedance network components are symmetrical i.e. the inductors L_1 and L_2, and capacitors C_1 and C_2 are equal (L_1=L_2=L and C_1=C_2=C). Therefore, the inductor current and capacitor voltage are identical. Furthermore, the parasitic resistor of the inductors is considered in the inverter model. This inverter has three operating intervals over a complete duty cycle. In the first interval (T_{ON}), the switches Q_1 and Q_4 are conducted in a positive active switching state. During the second interval (T_{OFF}), the switches Q_2 and Q_3 are conducted in a negative active switching state. Finally, the third interval (T_{ST}) is related

to the shoot-through (ST) switching state that all switches are turned on simultaneously to boost the input voltage. According to the z-source converter operation and considering the inductor volt-seconds balance, the following relations are established in ZSI [10]:

$$V_{C1} = V_{C2} = V_C = \frac{1 - D_{ST}}{1 - 2D_{ST}} \times V_{DC} \tag{1}$$

$$V_{INV} = 2V_C - V_{DC} = \frac{1}{1 - 2D_{ST}} \times V_{DC}, \tag{2}$$

where D_{ST} is the shoot-through duty cycle ($D_{ST}= T_{ST}/T$). To obtain the state-space of the ZSI, the average model of the operation modes is considered in this paper. To this end, according to the operation modes of ZSI, the average of three different state-space are evaluated:

$$\dot{X} = A_{AVG}X + B_{AVG}U\ , \tag{3}$$

where X is the inductor current and capacitor voltage of impedance network, and inductor current of inverter AC side as the state variables, $X=[I_{L1}, V_{C1}, I_{LS}]$, and U is the input DC voltage and grid voltage, $U=[V_{DC}, V_{Grid}]$. Moreover, the A_{AVG} and B_{AVG} are defined as (A_{AVG}, A_{ON}, A_{OFF}, A_{ST}, B_{AVG}, B_{ON}, B_{OFF}, and B_{ST} are matrices):

$$A_{AVG} = \frac{1}{T}\left(T_{ON}A_{ON} + T_{OFF}A_{OFF} + T_{ST}A_{ST}\right) \tag{4}$$

$$B_{AVG} = \frac{1}{T}\left(T_{ON}B_{ON} + T_{OFF}B_{OFF} + T_{ST}B_{ST}\right), \tag{5}$$

where $T_{ON}=(\mu_m+1-D_{ST}/2)\times T$, $T_{OFF}=(1-T_{ON}-T_{ST})$, and μ_m is amplitude modulation index. To obtain the state-space of ZSI, presented in Fig 1, the ZSI is simplified into two separated systems. The H-bridge, L_S, and grid are considered a simple switch and constant current source (I_S) in the first system. Therefore, the first system consists of the input voltage source, impedance network, and equivalent circuit of the switch and current source. Moreover, the second system involves the constant DC voltage (V_{INV}), H-bridge, grid impedance, and grid voltage. In [11-12], the state-space ZSI is analyzed with a similar procedure. Accordingly, the state-space of ZSI is obtained as:

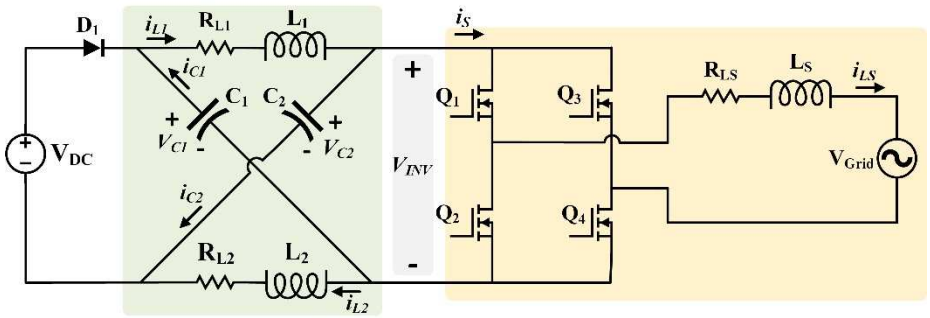

Fig. 1: Single-phase grid-connected z-source inverter

$$\begin{bmatrix} \dot{i}_{L1} \\ \dot{v}_{C1} \end{bmatrix} = \begin{bmatrix} \frac{-R_{L1}}{L} & -\frac{1}{L} + \frac{2}{L}D_{ST} \\ -\frac{1}{C} + \frac{2}{C}D_{ST} & 0 \end{bmatrix} \begin{bmatrix} i_{L1} \\ v_{C1} \end{bmatrix} + \begin{bmatrix} \frac{(2D_{sh} - 1)V_{DC} - 2R_{L1}I_S}{L(2D_{ST} - 1)^2} \\ \frac{2I_S}{C(2D_{ST} - 1)} \end{bmatrix} d_{ST} \tag{6}$$

$$\left[\dot{i}_{LS}\right]=\left[-\frac{R_{LS}}{L_S}\right]\left[i_{LS}\right]+\left[\frac{2V_C-V_{DC}}{L_S}\right]\mu_m \tag{7}$$

Therefore, the small-signal analysis can be performed in order to obtain the transfer functions of ZSI:

$$G_1(s)=\frac{i_L}{D_{ST}}=\frac{C\left(V_{DC}-2D_{ST}V_{DC}-2I_S r_L\right)s+\left(2-8D_{ST}+8D_{ST}^2\right)I_S}{\left(2D_{ST}-1\right)^2\left(C\,L\,s^2+C\,r_L\,s+4D_{ST}^2-4D_{ST}+1\right)} \tag{8}$$

$$G_2(s)=\frac{v_C}{D_{ST}}=\frac{\left(2D_{ST}-1\right)\left(2I_S L\,s+4I_S r_L-(1-2D_{ST})V_{DC}\right)}{C\left(V_{DC}-2D_{ST}V_{DC}-2I_S r_L\right)s+2I_S+8D_{ST}^2 I_S-8D_{ST}I_S} \tag{9}$$

$$G_3(s)=\frac{i_{L_S}}{\mu_m}=\frac{2V_C-V_{DC}}{L_S\,s+r_{L_S}} \tag{10}$$

In $G_1(s)$ to $G_3(s)$, capital letters represents the variables at the operating point. Therefore, I_S and V_{DC} are the constant value at the operating point. As it can be seen, $G_2(s)$ represents a non-minimum phase system due to the existing RHP zero into the transfer function. Fig. 2 represents the pole and zero trajectories of control-to-capacitor with system parameter variations (C is considered constant and L is varied). Consequently, a MIMO ZSI is presented that the input variables (control variables) are shoot-through duty cycle (D_{ST}) and amplitude modulation index (μ_m), and the outputs are capacitor voltage of DC side and inductor current of inverter AC side.

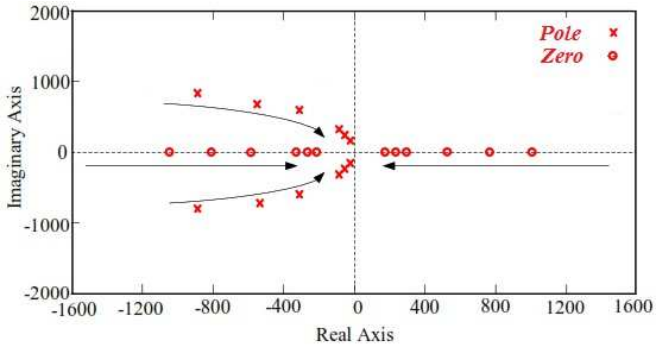

Fig. 2: Pole and zero trajectories with system parameters variations

Proposed neural networks-generalized predictive model

The GPC algorithm is exploited based on the transfer function that can possibly be a non-minimum phase and unstable system by considering the challenges regarding disturbances and noises. In MPC algorithms, the response is consists of free response and forced response. The free response refers to the signals in the past, and the forced response is related to the signals in the future. In this paper, controlled auto-regressive integrated moving average (CARIMA) is used to model the system in GPC:

$$A(z^{-1})y(t)=z^{-d}B(z^{-1})u(t-1)+C(z^{-1})\frac{e(t)}{(1-z^{-1})} \tag{11}$$

where d is the system delay, e(t) is the noise that in this paper noise is not considered into the model, and $A(z^{-1})$ and $B(z^{-1})$ are obtained from the discrete-time model of transfer functions:

$$A(z^{-1})=1+a_1z^{-1}+a_2z^{-2}+\ldots+a_nz^{-n_a} \tag{12}$$

$$B(z^{-1})=b_0+b_1z^{-1}+b_2z^{-2}+\ldots+b_nz^{-n_b} \tag{13}$$

According to the Diophantine equation in (13), the $E(z^{-1})$ and $F(z^{-1})$ can be calculated as a recursive relationship in (14) and (15) in order to predict the signals:

$$E_j(z^{-1})(1-z^{-1})\,A(z^{-1})+z^{-j}F_j(z^{-1})=1 \tag{14}$$

$$E_{j+1}(z^{-1})=E_j(z^{-1})+f_{j,0}z^{-j} \tag{15}$$

$$f_{j+1,i}=f_{j,i+1}-f_{j,0}\tilde{a}_{i+1} \qquad i=0,1,...,n_{\tilde{a}}-1\ , \tag{16}$$

where j is the prediction horizon, and i represents the corresponding terms of the $F_j(z^{-1})$. In addition, $\tilde{a}_i$ is i th term of $(1–z^{-1})A(z^{-1})$. Therefore, according to (10) and considering $e(t)$=0, the estimated outputs at the predictive horizon can be obtained:

$$\hat{y}(t+j\,|\,t)=B(z^{-1})E_j(z^{-1})(1-z^{-1})u(t+j-d-1)+F_j(z^{-1})y(t) \tag{17}$$

In (16), $F_j(z^{-1})y(t)$ is dependent on the past control signals. However, $B(z^{-1})E_j(z^{-1})(1-z^{-1})u(t+j-d-1)$ is included both past and future control signals. In conventional GPC, the free response and forced response are separated by the following equation:

$$y=\Phi y_{\_}+\Pi u_{\_}+\Omega u \tag{18}$$

The first two terms in (17) are related to the past control signals, and the third term is related to the future control signals. The matrixes Φ , Π , and Ω are defined as below in the conventional GPC algorithm:

$$\Phi=\begin{bmatrix} f_{d+1,0} & \cdots & f_{d+1,n_a} \\ \cdots & \cdots & \cdots \\ f_{d+N,0} & \cdots & f_{d+N,n_a} \end{bmatrix} \quad \Pi=\begin{bmatrix} g_{d+1,1} & \cdots & g_{d+1,n_{g1}} \\ \cdots & \cdots & \cdots \\ g_{d+N,N} & \cdots & g_{d+N,n_{gN}} \end{bmatrix} \quad \Omega=\begin{bmatrix} g_{d+1,0} & 0 & 0 \\ \cdots & \cdots & \cdots \\ g_{d+N,N-1} & \cdots & g_{d+N,0} \end{bmatrix} \tag{19}$$

In the proposed NN-GPC algorithm, the forced response presented as Ωu in conventional GPC is replaced with feed-forward neural networks in order to predict the control signals. Therefore, the Ω matrix components are obtained by NN. In this algorithm, the GPC calculations reduce, instead the neural networks calculations are put in the algorithm. Fig. 3 represents the NN structure to predict the state variables. More accurate predicted state variables for the GPC enhance the algorithm operation and dynamic response of the ZSI. Fig. 4 shows the proposed NN-GPC. The inductor current and capacitor voltage of the impedance network and inductor current of inverter AC side as the feedback signals are inputs of the feed-forward NN and GPC. After algorithm calculations, the cost function units evaluate the optimum output control signals according to the predicted signals and reference signals. Eventually, the output control signals are applied to the gate drive to switch on or off the switches.

The cost function can be define as:

$$CF=(R-Y)^T(R-Y)+\alpha u^T u\ , \tag{20}$$

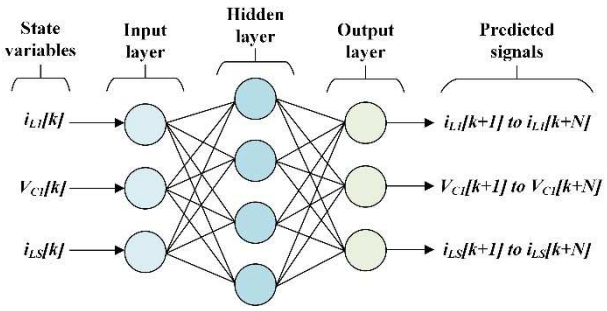

Fig. 3: Neural networks structure to predict the control signals

where R is the reference values $R=[R(t+d+1), R(t+d+2), ..., R(t+d+N)]$, Y is defined in (17), and α is a constant value. Therefore, the optimum control signal can be stated:

$$u = (\Omega^T \Omega + \alpha I)^{-1} \Omega^T (R - \Phi y_{\_} - \Pi u_{\_}) \tag{21}$$

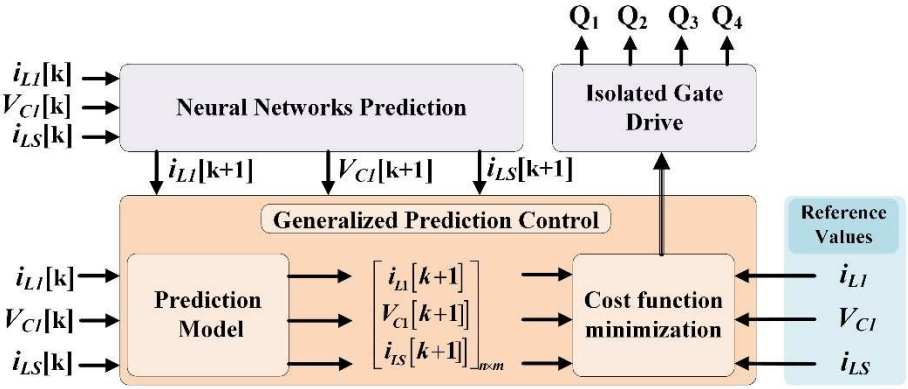

Fig. 4: Proposed NN-GPC

Performance evaluation and simulation results:

To evaluate the performance of the proposed NN-GPC on ZSI control, a ZSI with the specifications in Table I is considered. The NN is trained offline based on the obtained data of the ZSI simulation performance. Consequently, the NN offers the components of matrix Ω that are related to the future signals according to the instant values of state variables. On the other hand, the GPC algorithm evaluates the components of the matrices Φ and Π that are basically referred to the past signals. The NN parameters and GPC algorithm parameters are presented in Table I.

In order to evaluate the ZSI operation with the proposed NN-GPC, the simulation is carried out in MATLAB/ SIMULINK, and the results are compared with the conventional GPC. The neural networks toolbox is utilized to predict the state variables, and the GPC is set up by MATLAB codes. Eventually, the output signals of the cost function minimization are applied to the gate driver. The switching method in this simulation is the unipolar method. Figure 5 and 6 show the capacitor voltage and inductor current of the impedance network, coupling inductor current (L_S), and H-bridge inverter input voltage. It can be observed that the state variables follow their reference values effectively. In order to evaluate the dynamic response of ZSI in transients, the output current reference at 0.1ms is changed from 10A to 20A. The performance of NN-GPC and conventional GPC in transient can be seen in Fig. 5 and 6. The state variables in the conventional GPC are not able to trace the reference values in transition when the current reference is changed. However, the accurate prediction of state variables by feed-forward NN in NN-GPC makes the voltages and current track the reference values effectually. Although the MPC-GPC is also shown a favorable result in general specially comparing with PID controller, the proposed NN-GPC presents an effective performance specifically from the dynamic response perspective. Table II represents a characteristics comparison of GPC and NN-GPC.

Table I: Z-source inverter and NN-GPC specifications

ZSI parameters		NN-GPC parameters		
V_{DC}	100Vdc	**NN specifications**	Input Data	3×100
V_{Grid}	110Vrms		Output Data	3×100
C_1 & C_2	1mF		Training	70%
L_1 & L_2	5.1mH		Validation	15%
R_{L1} & R_{L2}	0.25Ω		Testing	15%
L_S	5.1mH		No. Hidden Neurons	3
R_{Ls}	0.25Ω	**GPC specifications**	Sample T	2μs
I_{OUT}	20A		Predictive horizon	4
$VC_{1\text{-ref}}$	230V		Control horizon	4

Table II: Comparison of GPC and NN-GPC characteristics

Specification	GPC	NN-GPC
System control	- Linear system - Nonlinear system - Minimum phase system - Non-minimum phase system	- Linear system - Nonlinear system - Minimum phase system - Non-minimum phase system
Complexity	Lower	Higher
Dynamic response	Lower	Higher

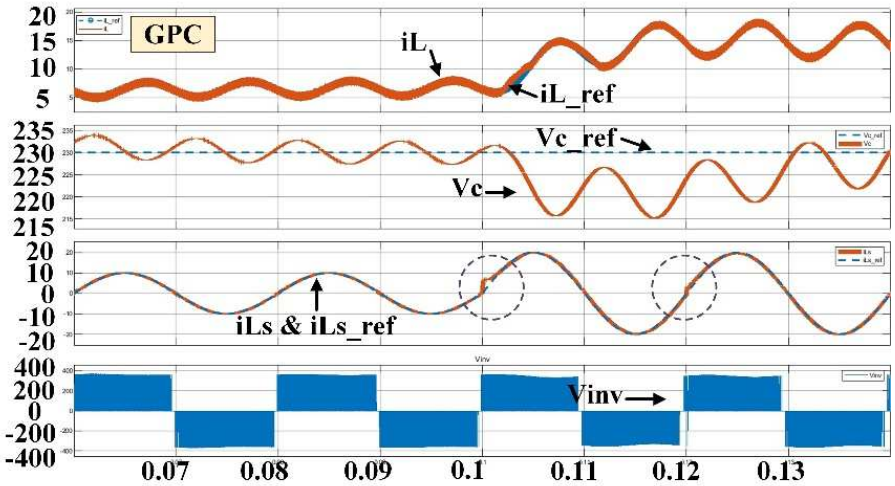

Fig. 5: Simulation results of ZSI control by GPC

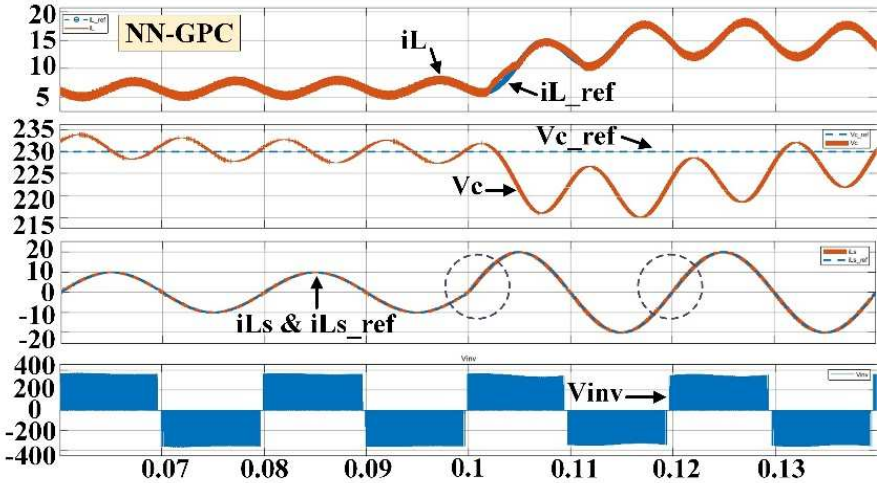

Fig. 6: Simulation results of ZSI control by NN-GPC

Conclusion

In this paper, an NN-GPC algorithm is proposed in order to control a ZSI. As discussed, the ZSI has non-minimum phase characteristics due to existing RHZ zero in control to capacitor voltage transfer function. Therefore, conventional linear control methods such as PID controllers make the ZSI operation unreliable and inefficient. The MPC algorithms as a promising control method for non-linear and non-minimum phase systems is considered recently to optimum control of ZSI. Eventually, the GPC algorithm is applied in this paper according to the MIMO model of ZSI. By deploying a feed-forward NN and improving the system identification to predict the state variables of the converter, the performance of the GPC algorithm is enhanced. Eventually, the simulation results for a specific ZSI are presented to verify the proposed NN-GPC algorithm.

Funding

Grant PGC2018-098946-B-I00 funded by: MCIN/ AEI /10.13039/501100011033/ and by ERDF ERDF A way of making Europe.

References

[1] Hasan Babayi Nozadian, Mohsen, et al. "Switched Z-source networks: a review." IET Power Electronics 12.7 (2019): 1616-1633.
[2] Nguyen, Minh-Khai, Young-Cheol Lim, and Sung-Jun Park. "Improved trans-Z-source inverter with continuous input current and boost inversion capability." IEEE transactions on power electronics 28.10 (2013): 4500-4510.
[3] Salehi, Navid, Herminio Martínez-García, and Guillermo Velasco-Quesada. "Modified Cascaded Z-Source High Step-Up Boost Converter." Electronics 9.11 (2020): 1932.
[4] Ellabban, Omar, Joeri Van Mierlo, and Philippe Lataire. "A comparative study of different control techniques for an induction motor fed by a Z-source inverter for electric vehicles." 2011 International Conference on Power Engineering, Energy and Electrical Drives. IEEE, 2011.
[5] Ding, Xinping, et al. "A direct DC-link boost voltage PID-like fuzzy control strategy in Z-source inverter." 200
8 IEEE Power Electronics Specialists Conference. IEEE, 2008.
[6] Rostami, H., and D. A. Khaburi. "Neural networks controlling for both the DC boost and AC output voltage of Z-source inverter." 2010 1st Power Electronic & Drive Systems & Technologies Conference. IEEE, 2010.
[7] Bakeer, Abualkasim, et al. "Control of switched-inductor quasi Z-Source Inverter (SL-qZSI) based on model predictive control technique (MPC)." 2015 IEEE International Conference on Industrial Technology. IEEE, 2015.
[8] Sajadian, Sally, and Reza Ahmadi. "Model predictive control of dual-mode operations Z-source inverter: Islanded and grid-connected." IEEE Transactions on Power Electronics 33.5 (2017): 4488-4497.
[9] Xu, Yuhao, et al. "Model Predictive Control Using Joint Voltage Vector for Quasi Z-Source Inverter with Ability of Suppressing Current Ripple." IEEE Journal of Emerging and Selected Topics in Power Electronics (2021).
[10] Peng, Fang Zheng. "Z-source inverter." IEEE Transactions on industry applications 39, no. 2 (2003): 504-510.
[11] Zakipour, Adel, Shokrollah Shokri-Kojori, and Mohammad Tavakoli Bina. "Sliding mode control of the nonminimum phase grid-connected Z-source inverter." International Transactions on Electrical Energy Systems 27, no. 11 (2017): e2398.
[12] Loh, Poh Chiang, D. Mahinda Vilathgamuwa, Chandana Jayampathi Gajanayake, Yih Rong Lim, and Chern Wern Teo. "Transient modeling and analysis of pulse-width modulated Z-source inverter." IEEE Transactions on Power Electronics 22, no. 2 (2007): 498-507.